

Measurement of the Curie temperature distribution in FePt granular magnetic media

S. Pisana, S. Jain, J. W. Reiner, G. J. Parker, C. C. Poon, O. Hellwig, and B. C. Stipe

Citation: [Applied Physics Letters](#) **104**, 162407 (2014); doi: 10.1063/1.4873543

View online: <http://dx.doi.org/10.1063/1.4873543>

View Table of Contents: <http://scitation.aip.org/content/aip/journal/apl/104/16?ver=pdfcov>

Published by the [AIP Publishing](#)

Articles you may be interested in

[Simulations of magnetic hysteresis loops at high temperatures](#)

J. Appl. Phys. **116**, 123910 (2014); 10.1063/1.4896582

[Effects of grain microstructure on magnetic properties in FePtAg-C media for heat assisted magnetic recording](#)

J. Appl. Phys. **113**, 043910 (2013); 10.1063/1.4788820

[The Curie temperature distribution of FePt granular magnetic recording media](#)

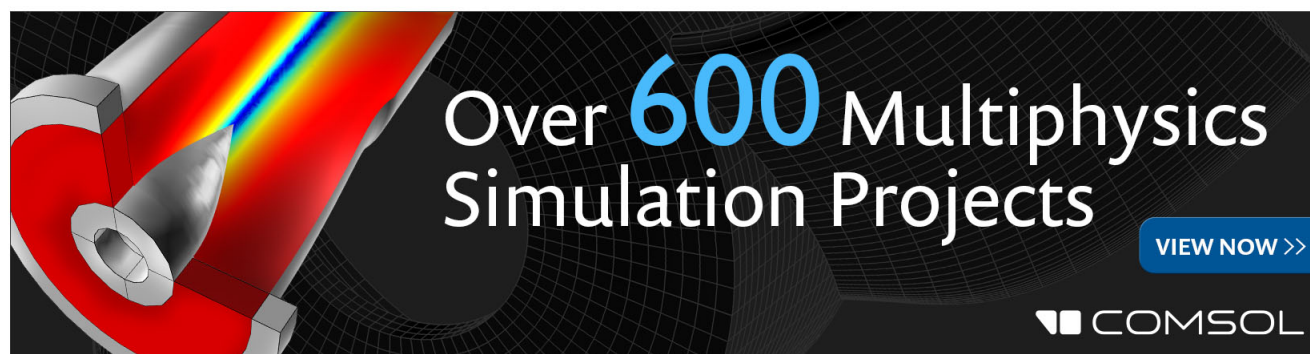
Appl. Phys. Lett. **101**, 052406 (2012); 10.1063/1.4740075

[Hard/graded exchange spring composite media based on FePt](#)

J. Appl. Phys. **109**, 07B729 (2011); 10.1063/1.3556773

[Fabrication and magnetic properties of nanopatterned FePt media](#)

J. Appl. Phys. **99**, 08G909 (2006); 10.1063/1.2166599

The advertisement for COMSOL Multiphysics features a dark background with a grid pattern. On the left, there is a 3D model of a mechanical part with a red and yellow color gradient. The text 'Over 600 Multiphysics Simulation Projects' is prominently displayed in the center in a large, white, sans-serif font. To the right of this text is a blue button with the text 'VIEW NOW >>'. In the bottom right corner, the COMSOL logo is visible, consisting of a small square icon followed by the word 'COMSOL' in a white, sans-serif font.

Measurement of the Curie temperature distribution in FePt granular magnetic media

S. Pisana,^{a)} S. Jain, J. W. Reiner, G. J. Parker, C. C. Poon, O. Hellwig, and B. C. Stipe
 HGST, A Western Digital Company, San Jose Research Center, San Jose, California 95135, USA

(Received 27 January 2014; accepted 16 April 2014; published online 25 April 2014)

Heat assisted magnetic recording (HAMR) has been recognized as a leading technology to increase the data storage density of hard disk drives. Dispersions in the properties of the grains comprising the magnetic medium can lead to grain-to-grain Curie temperature variations, which drastically affect the jitter in the recorded magnetic transitions and limit the data storage density capabilities in HAMR. Here we present a method to measure the switching probability of an ensemble of exchange-decoupled grains with perpendicular anisotropy subject to nanosecond heating pulses. The short heat exposure time ensures that the grains switch by reaching the Curie temperature rather than through thermal activation. The switching probability can be directly interpreted as representing the Curie temperature distribution. The method is applied to two sets of samples to reveal the sensitivity of the Curie temperature distribution to FePt HAMR media fabrication parameters. This technique is of importance to engineer suitable HAMR media capable of high density magnetic recording and for fundamental studies on sources of magnetic disorder in granular magnetic media. © 2014 AIP Publishing LLC. [<http://dx.doi.org/10.1063/1.4873543>]

The introduction of heat assisted magnetic recording (HAMR) as a future generation magnetic recording technology is catalyzed by the potential data storage areal density gain expected by reducing the grain size of the magnetic grains comprising the storage medium,¹ and by increasing the effective write field gradient from the recording head $\partial H_k / \partial x$ through a combination of large anisotropy field gradient $\partial H_k / \partial T$ and thermal gradient $\partial T / \partial x$.² The variance in bit transition position in the recorded data (known as jitter) is an important performance parameter governing the data storage capability of a recording medium. In HAMR, jitter is currently dominated by Curie temperature, grain temperature, and anisotropy field distributions (referred to σ_{T_c} , σ_T , and σ_{H_k} , respectively).^{3,4} Conventional factors such as the number of grains per bit and grain size distribution also play a role. Though both σ_{T_c} and σ_T have the same effect on jitter,⁴ the former is caused by variations in intrinsic grain properties, whereas the latter is caused by extrinsic variations in thermal coupling efficiency with the heat source or the substrate. Zhu calculated the impact on medium signal to noise ratio of $\sigma_{T_c} = 5\%$ or $\sigma_T = 5\%$ to be equal to $\sigma_{H_k} = 30\%$,^{3,4} highlighting the strong detrimental impact of small σ_{T_c} and σ_T distributions.

There are several potential origins to a T_c distribution, such as variations in grain composition, chemical ordering, size and strain.^{5–7} These effects need to be investigated in order to minimize jitter in HAMR. Techniques have been identified to characterize σ_{H_k} in granular media,^{8–12} however no approach to measure σ_T in a HAMR recording system has so far been reported. Similarly, there are no reported approaches to measure σ_{T_c} in granular media. This should not be confused with known methods to measure the Blocking temperature distribution σ_{T_b} .^{13–15} The Blocking temperature represents the temperature below which the

grain switching probability is essentially zero due to lack of sufficient thermal energy or external magnetic field to overcome the energetic barrier to switching. The Blocking temperature is therefore a function of several magnetic and physical properties of the grain, as well as external factors such as applied field magnitude and angle, and the characteristic time of measurement which for typical magnetometry techniques is of the order of several seconds. σ_{T_b} is related to σ_{T_c} , but attempts to relate the two quantities would require assumptions or measurements of all of the related parameters and related distributions, such as grain volume and magnetocrystalline anisotropy energy density (K_u).

Here we report on an approach to directly measure σ_{T_c} , which is particularly suited to ensembles of exchange-decoupled grains with aligned anisotropy axes and remanent magnetization. The technique employs a pulsed laser source to heat the grains to their Curie temperature under a uniformly applied magnetic field. The temperature excursion is short enough for the grain switching temperature to approach T_c . The applied magnetic field strength is kept below the threshold to switch the grains at room temperature or by thermal activation, but it is strong enough to deterministically switch the grains while cooling through T_c . A second laser is used to determine the fraction of switched grains through the polar Kerr effect. The experimental setup is shown in Fig. 1(a). A pulsed Nd:YLF laser operating at 1047 nm and 200 Hz (LWE-110) is used as the pump. To maximize pulse energy stability, the laser is kept at constant power with a free-running pulse train. Single pulses are obtained by triggering a fast mechanical shutter, and fine pulse energy control is obtained through a liquid crystal variable retarder (LCVR) and polarizer. A pulse energy meter samples a fraction of the pump light. A continuous wave laser operating at 640 nm is used as a probe (Coherent Cube). Pump, probe and white light are focused on the sample using an achromat between the poles of an electromagnet. The optical system is

^{a)}Electronic mail: simone.pisana@hgst.com

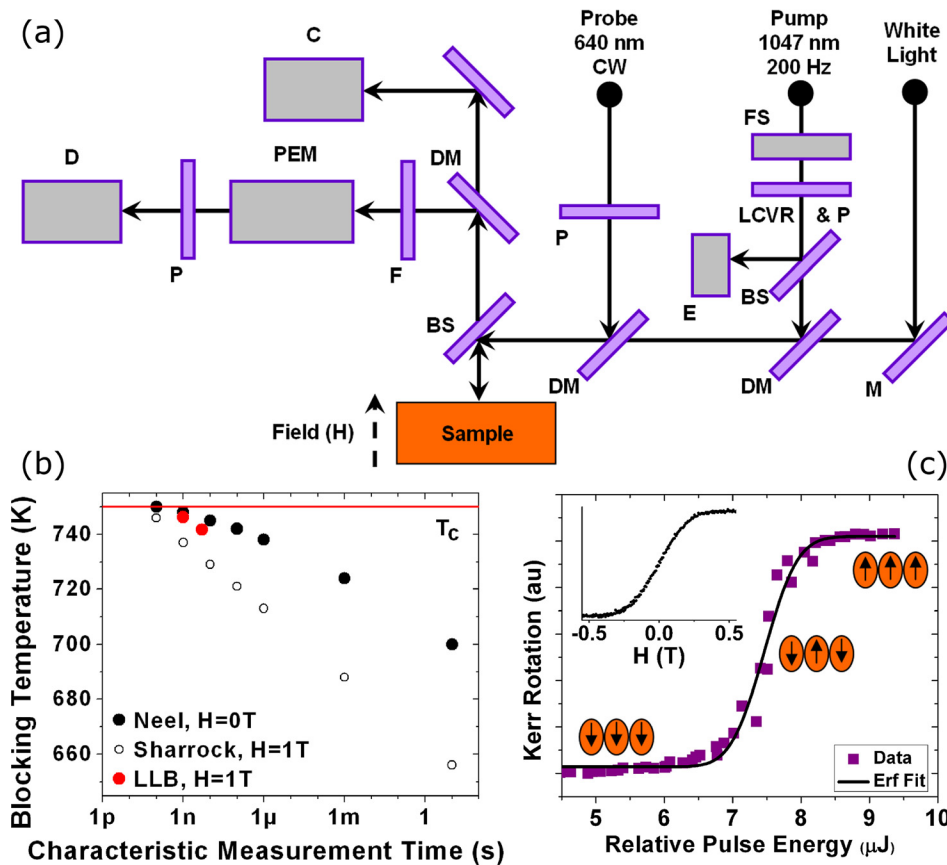


FIG. 1. (a) Schematic diagram of the experimental setup for measurement of Curie temperature distribution. The labels indicate mirrors (M), dichroic mirrors (DM), beam splitters (BS), fast shutter (FS), polarizers (P), LCVR, pulse energy meter (E), filter (F), photo-elastic modulator (PEM), detector (D), and camera (C). The sample focusing achromat and camera tube lens are not shown. (b) Models of grain switching temperature as a function of characteristic measurement time. As the measurement time reduces, the blocking temperature reaches the Curie temperature. (c) Example of a measured switching probability as a function of relative grain temperature. The number of switched grains is measured by Kerr rotation, and the grain temperature is linearly proportional to the pump pulse energy. The schematics represent the grain magnetization direction as the temperature is increased. The inset shows a M-H magnetization curve measured by Kerr rotation where for each field value a pump pulse of saturating energy was applied.

designed to obtain a pump/probe beam diameter aspect ratio of 12 (beam diameters at $1/e^2$ are $65.4 \mu\text{m}$ and $5.5 \mu\text{m}$ for the pump and probe, respectively). This ensures that the probed grains are uniformly heated by the pump.²⁴ The probe light is analyzed through a photoelastic modulator (Hinds Instruments) to determine the Kerr rotation. The pump, probe, and white light are also focused on a camera for inspection. The coaxial pump to probe alignment and accuracy of focus is carefully calibrated as these can contribute to errors in determining σ_{T_c} .

To help illustrate how the presented approach samples σ_{T_c} , we compare the switching temperature of the grains under different experimental conditions. A Néel relaxation model of a grain was used to compare the Blocking temperature to the Curie temperature¹³ in zero applied magnetic field

$$T_b = \frac{K_u(T)V}{k_B \ln(f_0 t)}, \quad (1)$$

where V is the volume of a $7 \times 10 \text{ nm}$ cylindrical grain, k_B is Boltzmann's constant, $f_0 = 10^{10} \text{ Hz}$ is the attempt frequency, and t is the characteristic measurement time. The temperature dependence of the anisotropy was incorporated as $K_u(T) = K_u(0)(M(T)/M(0))^{2.1}$, where $K_u(0) = 4.5 \times 10^7 \text{ erg/cc}$ and $M(T) = M(0)(1 - T/T_c)^{1/3}$ is the temperature dependence of the magnetization.^{2,20,21,23} The result assuming a grain $T_c = 750 \text{ K}$ is shown in Fig. 1(b). For this case, the characteristic measurement time is the time within which one observes a grain's magnetization: the longer it is, the higher the chance for a switching event to take place. As shown in the figure, at 700 K the grain's magnetization can switch spontaneously in 10 s . Only if the characteristic

measurement time is of the order of 1 ns does the switching temperature approach T_c . Applying an external reversing magnetic field will further reduce the switching time, as this lowers the potential barrier for the magnetization to switch. The case of an applied magnetic field of 1 T can be estimated through Sharrock's formula.¹⁶ Here the characteristic measurement time represents the length of time an external magnetic field is applied for in order to switch the grain at a given temperature. Conversely, the result can be interpreted as the length of time a given temperature is applied in order to switch the grain at the applied external field of 1 T . As seen in the figure, an external applied field of 1 T allows the magnetization to switch at lower temperatures, so the field pulse would have to be shorter than 100 ps for the switching temperature to approach T_c . These statistical models oversimplify the switching physics at high temperature and depend heavily on the choice of f_0 . A more realistic model based on the Landau-Lifshitz-Bloch (LLB) equation for an ensemble of typical FePt grains was also employed to verify the behavior.¹ The LLB model's result shows that in order to sample grains switching near T_c , the characteristic measurement time needs to approach the nanosecond time scale. Since nanosecond magnetic field pulses of sufficient strength are impractical, a pulsed laser is used here to rapidly heat and cool the grains. The pulsed pump laser used in this work delivers 6 ns pulses. In order to calculate the length of time the grains are exposed to elevated temperatures after a pump pulse, we use a finite element model (FEM) of the optical absorption and thermal transport in our samples. The model incorporates the optical far-field measurement geometry in our setup, the pump pulse's temporal profile and spot size,

and the optical and thermal properties of all the layers and interfaces comprising the magnetic medium as determined by spectroscopic ellipsometry or time-domain thermoreflectance,²² respectively. We find that the length of time the grains stay within 50 K of the peak temperature is <10 ns. Therefore, the pulsed pump excitation is rapid enough to allow us to detect grain switching events at temperatures within 1% of T_c . The optical and thermal model also verifies that the grain temperature is linear with pump pulse energy, and that for our measurements on FePt granular media the measurement is insensitive to σ_T , the distribution in grain temperatures due to differences in optical absorption or thermal coupling to the substrate.

To measure σ_{T_c} , we use the following measurement procedure to obtain the switching temperature distribution in Fig. 1(c). While applying a constant magnetic field, the pump laser energy level is swept from zero to a point where all the grains in the medium switch. For each pump laser energy level, the magnetic grains are re-initialized to a uniformly magnetized state (for example, in the down direction, as schematically shown in Fig. 1(c)) by applying a sufficiently strong pump laser pulse in a constant magnetic field of opposite polarity. The Kerr rotation can be measured in the remanent state or in a field below the room temperature nucleation field. The upper limit of the pump laser pulse energy is chosen to saturate the switching behavior and is well below the threshold for which structural and magnetic damage occurs. Media damage can be first detected by irreversible changes in the magnetization, followed by structural changes that can be seen on the camera or by atomic force microscopy (AFM) analysis. The magnetic field strength used in the experiment is sufficiently strong to deterministically switch the grains, but below the room temperature nucleation field. For example, for our FePt HAMR media, a field of 5–10 kOe is too weak to switch the grains at room temperature, but strong enough to switch all the grains as they cool through T_c . The inset in Fig. 1(c) shows a Kerr magnetization loop in which at each applied field value a saturating pump pulse is applied. As seen, the curve follows a Brillouin lineshape and indicates that for saturating pump pulse energies all the grains switch at fields above 5 kOe, and a demagnetized state is obtained at zero field. As one would expect, the total Kerr rotation in the switching temperature distribution curve is decreased by exactly 1/2 if the applied field is zero, representative of a demagnetized state where the grains randomly orient along the anisotropy axis upon cooling from T_c in zero field.

The data of Fig. 1(c) shows some scatter in the transition region. This is not primarily due to noise in the Kerr measurement, but rather it originates from the sharpness of the transition and finite uncertainty in the pump pulse energy.²⁵ To minimize errors due to uncertainties in laser pulse energies, each data point collected is the median result of five independent measurements at the same nominal pulse energy.²⁶ The re-initialization of the grains to a uniformly magnetized state after each pump pulse is also helpful to more accurately resolving the transition. If the measurement were to be carried out without magnetic re-initialization of the grains, the sharpness of the transition in the measured grain switching probability would be dominated by high

pulse energy outliers, which would account for most of the reversal.

In order to obtain σ_{T_c} from the switching temperature distribution, we fit the data to a Gaussian Error function by assuming a random source of T_c variation. The fit yields the Curie temperature distribution expectation value (P_{50} , the point in which 50% of the grains have switched) and standard deviation (σ_{Energy}) in relative pulse energy units. We normalize these to obtain $\sigma_{Laser} = \sigma_{Energy}/P_{50}$, which represents the dispersion in laser energies necessary to switch the grains, and hence is a measure of the Curie temperature distribution. One can obtain σ_{T_c} if $\langle T_c \rangle$ is measured independently, for example by vibrating sample magnetometry (VSM)

$$\frac{\sigma_{T_c}}{\langle T_c \rangle} = \sigma_{Laser} \frac{\langle T_c \rangle - T_{amb}}{\langle T_c \rangle}, \quad (2)$$

where T_{amb} is the ambient temperature. As an example, fitting the data in Fig. 1(c) yields $\sigma_{Energy} = 0.384 \mu\text{J}$ and $P_{50} = 7.46 \mu\text{J}$, therefore $\sigma_{Laser} = 5.15\%$. Given a $\langle T_c \rangle = 742 \text{ K}$, as measured by VSM, we convert this to a $\sigma_{T_c} = 3.1 \pm 0.3\%$.

We now proceed to applying the measurement technique to two series of samples deposited with varying conditions (details of the deposition process¹⁷ and sample characterization⁸ have been reported previously). Fig. 2 shows the characterization of FePt granular media samples deposited at varying temperatures, which is expected to affect the mean chemical ordering of FePt. As the deposition temperature is increased, the X-ray diffraction (XRD) spectra show that the FePt (002) peak is shifting to higher angles and the (001)/(002) peak intensity ratio increases. Both of these metrics indicate that the FePt chemical order is increasing with temperature. This change is not accompanied by an appreciable increase in grain size, as determined by XRD in-plane coherence length or scanning electron microscopy (SEM) analysis. The magnetization loops indicate that the increase in chemical ordering is accompanied by enhanced anisotropy, which is evident as well by the increasing coercive field. Finally, Fig. 2(e) shows the measurements for σ_{Laser} , indicating a reduction in Curie temperature distribution as the deposition temperature is increased. Though the mean FePt ordering affects the mean Curie temperature of the grains,^{5,6} the σ_{Laser} variations in Fig. 2(e) normalize this out, since the switching temperature distribution is divided by the mean switching temperature. The σ_{Laser} trend can be explained in view of the thermodynamic drive for the FePt lattice to transform from a disordered fcc to an ordered $L1_0$ fct lattice, which increases at higher temperatures.¹⁸ As the deposition temperature increases, a larger fraction of the FePt grains will reach a thermodynamic equilibrium and therefore the grain ordering distribution is reduced. Given the 165 K difference in Curie temperature between the fcc and fct phases,⁵ a reduction in ordering distribution will translate in a reduction in σ_{T_c} .

Fig. 3 shows a second set of FePt granular media samples in which the sputtering pressure was varied. Due to the nature of the multi-target sputter source employed and the angular dependence of the sputter yield, variations in sputter pressure result in relative compositional variations in the

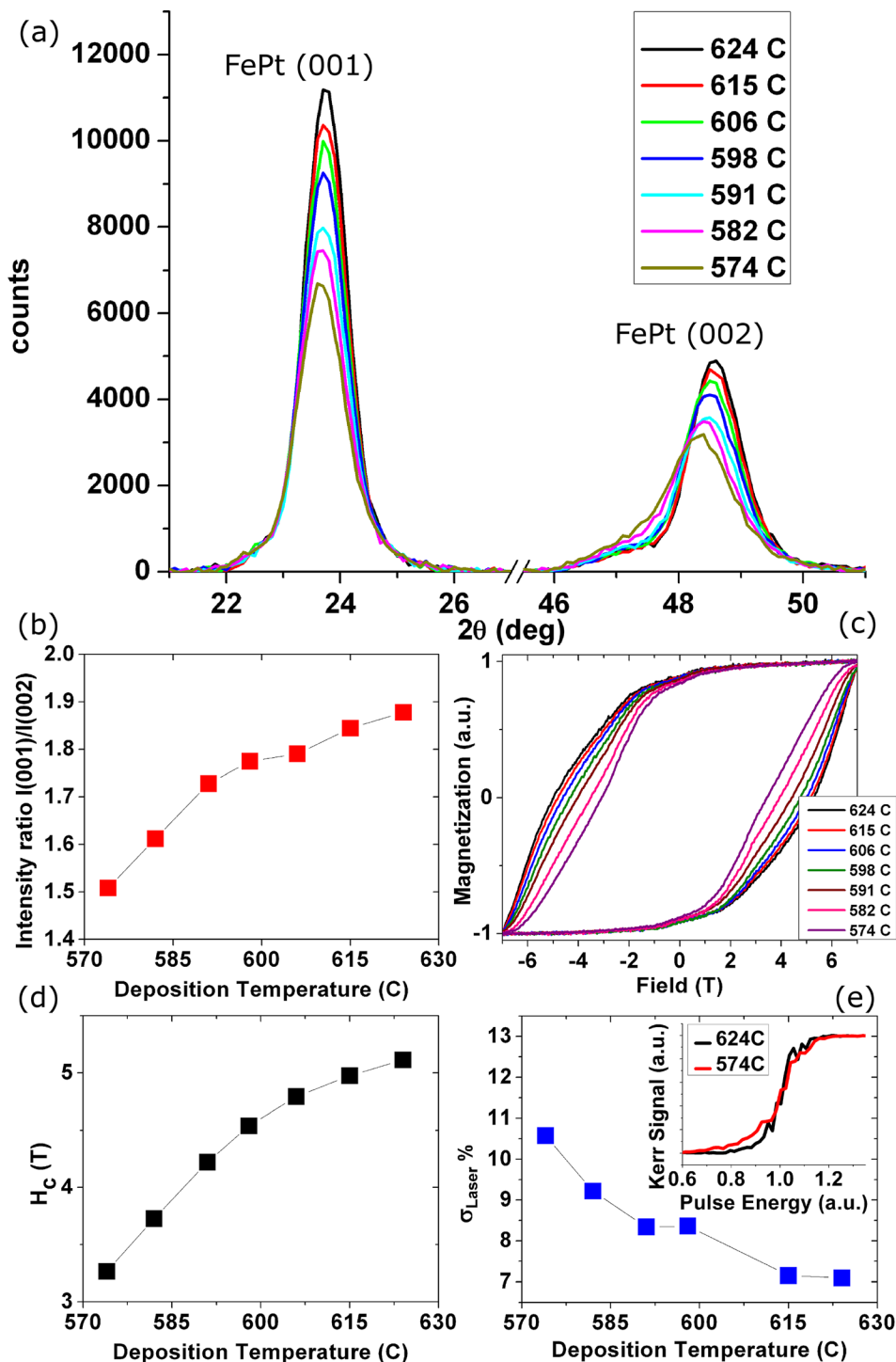


FIG. 2. (a) XRD 2θ scan focusing on the fundamental and superlattice FePt peaks as a function of deposition temperature. The integrated (001)/(002) peak intensity ratio (b), polar Kerr magnetization loops (c), coercivity (H_c) (d), and relative Curie temperature distribution (e) are plotted as function of deposition temperature. The inset in (e) shows the Curie temperature distribution measurements for two samples.

deposited FePt. Fig. 3(a) shows that pressure variations result in a linear trend in relative FePt composition, as determined by X-ray fluorescence (XRF) analysis, and also reflected in the XRD analysis of Fig. 3(b). A deposition pressure of 5 mTorr yields equiatomic FePt composition and optimized ordering. In this case no significant variation in grain size was found. The pressure dependence is also reflected in the magnetic properties. The magnetization is found to vary linearly with composition,¹ whereas anisotropy and coercivity are optimized at the equiatomic FePt composition.¹ The measurement of σ_{Laser} in Fig. 3(d) shows a pronounced reduction of Curie temperature distribution for equiatomic FePt composition. The trend in σ_{T_c} with relative FePt

composition can also be explained by the variation in ordering of the grains. The fcc to fct disorder/order transition temperature in the FePt phase diagram is minimized near equiatomic composition.¹⁹ As the transition temperature rises, the thermodynamic drive for phase transformation drops, leading to an increase in σ_{T_c} . Since the thermodynamic drive for phase transformation decreases away from equiatomic composition and the deposition temperature was not changed in these samples, lower values for σ_{T_c} may be attainable by further increasing the deposition temperature.

We have demonstrated a method to measure the Curie temperature distribution in magnetic granular media. The technique can be applied to ensembles of remanent and

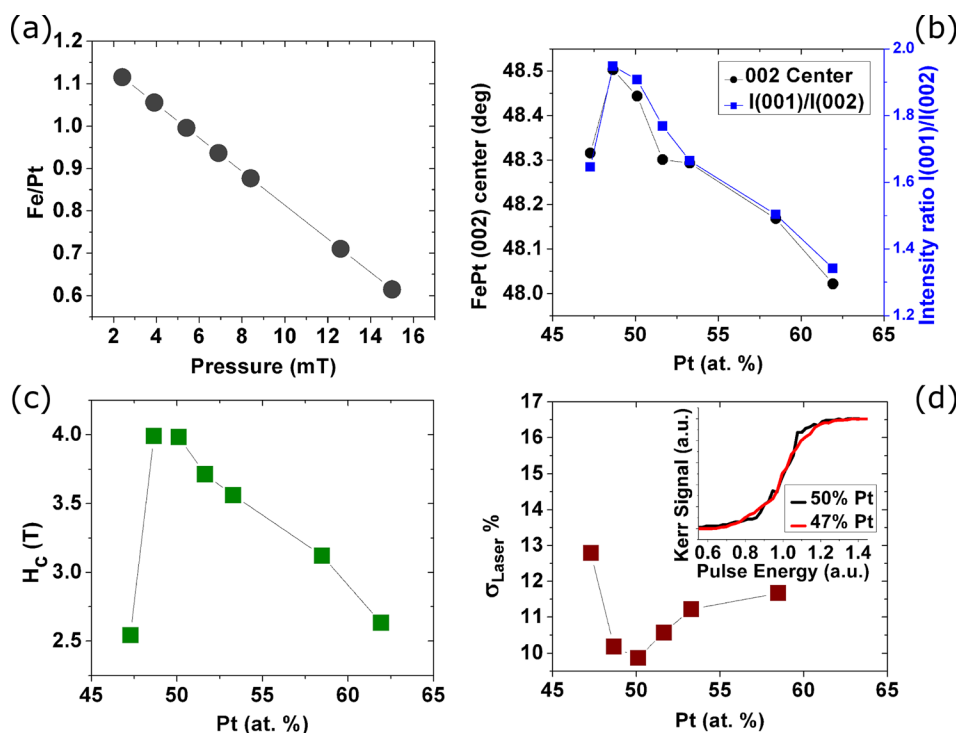


FIG. 3. Relative Fe/Pt grain composition determined by XRF as a function of gas pressure during deposition (a). XRD peak position and (001)/(002) peak intensity ratio (b), coercivity (H_c) (c), and relative Curie temperature distribution (d) are plotted as function of Pt content. The inset in (d) shows the Curie temperature distribution measurements for two samples.

magnetically decoupled grains with aligned anisotropy axis. Thanks to the rapid heating and cooling of the grains across the Curie temperature, this technique can also be employed to study the switching probability across the ferromagnetic phase transition as function of applied magnetic field strength and angle. Here we focus on FePt grains that are relevant to HAMR and show how maximizing the thermodynamic drive for $L1_0$ ordering reduces σ_{Tc} .

We thank Brian York and Henrik Zadoori for XRF characterization, Matteo Staffaroni for FEM simulation.

- ¹D. Weller, O. Mosendz, G. Parker, S. Pisana, and T. Santos, *Phys. Status Solidi A* **210**, 1245 (2013).
- ²J.-U. Thiele, K. R. Coffey, M. F. Toney, J. A. Hedstrom, and A. J. Kellock, *J. Appl. Phys.* **91**, 6595 (2002).
- ³H. Li and J.-G. Zhu, *IEEE Trans. Magn.* **49**, 3568 (2013).
- ⁴J.-G. Zhu and H. Li, *J. Appl. Phys.* **115**, 17B747 (2014).
- ⁵J. Lyubina, B. Rellinghaus, O. Gutfleisch, and M. Albrecht, *Handb. Magn. Mater.* **19**, 291 (2011).
- ⁶C.-b. Rong, D. Li, V. Nandwana, N. Poudyal, Y. Ding, Z. Wang, H. Zeng, and J. Liu, *Adv. Mater.* **18**, 2984 (2006).
- ⁷A. Lyberatos, D. Weller, G. J. Parker, and B. C. Stipe, *J. Appl. Phys.* **112**, 113915 (2012).
- ⁸S. Pisana, O. Mosendz, G. Parker, J. Reiner, T. Santos, A. McCallum, H. Richter, and D. Weller, *J. Appl. Phys.* **113**, 043910 (2013).
- ⁹S. Wicht, V. Neu, L. Schultz, D. Weller, O. Mosendz, G. Parker, S. Pisana, and B. Rellinghaus, *J. Appl. Phys.* **114**, 063906 (2013).

- ¹⁰C. Papusoi, K. Srinivasan, and R. Acharya, *J. Appl. Phys.* **110**, 083908 (2011).
- ¹¹A. Chernyshov, D. Treves, T. Le, C. Papusoi, H. Yuan, A. Ajan, and R. Acharya, *IEEE Trans. Magn.* **49**, 3572 (2013).
- ¹²H. Sakuma, T. Taniyama, Y. Kitamoto, Y. Yamazaki, H. Nishio, and H. Yamamoto, *J. Appl. Phys.* **95**, 7261 (2004).
- ¹³R. Chantrell, M. El-Hilo, and K. O'Grady, *IEEE Trans. Magn.* **27**, 3570 (1991).
- ¹⁴J. C. Denardin, A. L. Brandl, M. Knobel, P. Panissod, A. B. Pakhomov, H. Liu, and X. X. Zhang, *Phys. Rev. B* **65**, 064422 (2002).
- ¹⁵W. C. Nunes, W. S. D. Folly, J. P. Sinnecker, and M. A. Novak, *Phys. Rev. B* **70**, 014419 (2004).
- ¹⁶D. Weller and A. Moser, *IEEE Trans. Magn.* **35**, 4423 (1999).
- ¹⁷O. Mosendz, S. Pisana, J. W. Reiner, B. Stipe, and D. Weller, *J. Appl. Phys.* **111**, 07B729 (2012).
- ¹⁸D. C. Berry and K. Barmak, *J. Appl. Phys.* **101**, 014905 (2007).
- ¹⁹B. Wang and K. Barmak, *J. Appl. Phys.* **109**, 123916 (2011).
- ²⁰O. N. Mryasov, U. Nowak, K. Y. Guslienko, and R. W. Chantrell, *Europhys. Lett.* **69**, 805 (2005).
- ²¹O. Hovorka, S. Devos, Q. Coopman, W. J. Fan, C. J. Aas, R. F. L. Evans, X. Chen, G. Ju, and R. W. Chantrell, *Appl. Phys. Lett.* **101**, 052406 (2012).
- ²²A. J. Schmidt, X. Chen, and G. Chen, *Rev. Sci. Instrum.* **79**, 114902 (2008).
- ²³J. B. Staunton, S. Ostanin, S. S. A. Razee, B. L. Gyroff, L. Szunyogh, B. Ginatempo, and E. Bruno, *Phys. Rev. Lett.* **93**, 257204 (2004).
- ²⁴The finite size of the probe light would broaden the measurement if the grains $\sigma_{Tc} < 0.5\%$.
- ²⁵The laser source has a pulse energy stability of 1.5% at 1 σ .
- ²⁶This procedure can be simplified if the pump pulse energy of each shot can be monitored in real time with sufficient accuracy.